Structural Engineering and Mechanics, Vol. 5, No. 3 (1997) 239-256
DOI: http://dx.doi.org/10.12989/sem.1997.5.3.239

Rate-sensitive analysis of framed structures part II: implementation and application to steel and R/C frames

Q. Fang† and B.A. Izzuddin‡

Department of Civil Engineering, Imperial College, London SW7 2BU, U.K.

Abstract. The companion paper presents a new three-parameter model for the uniaxial rate-sensitive material response, which is based on a bilinear static stress-strain relationship with kinematic strain-hardening. This paper extends the proposed model to trilinear static stress-strain relationships for steel and concrete, and discusses the implementation of the new models within an incremental-iterative solution procedure. For steel, the three-parameter rate-function is employed with a trilinear static stress-strain relationship, which allows the utilisation of different levels of rate-sensitivity for the plastic plateau and strain-hardening ranges. For concrete, on the other hand, two trilinear stress-strain relationships are used for tension and compression, where rate-sensitivity is accounted for in the strain-softening range. Both models have been implemented within the nonlinear analysis program ADAPTIC, which is used herein to provide verification for the models, and to demonstrate their applicability to the rate-sensitive analysis of steel and reinforced concrete structures.

Key words: strain-rate effect; steel structures; reinforced concrete structures.

1. Introduction

The realistic prediction of the structural response under dynamic loading has become an important requirement for assessing existing structures, designing important new structures, and undertaking parametric investigations which lead to recommendations for design practice. Since the response of most materials is rate-sensitive, the behaviour of structural components under various dynamic loading conditions can only be predicted realistically if the effect of strain-rate on the material response is accounted for.

For steel and reinforced concrete structures subjected to severe dynamic loading conditions, such as impact, explosions and earthquakes, the strain-rate at critical regions within the structure can be as high as ($10\ \text{sec}^{-1}$). To predict the dynamic resistance of such structures, the constitutive properties of steel and concrete are required over a wide range of strain-rate. Soroushian and Choi (1987) presented the mechanical properties of steel at different strain-rates, ranging from ($10^{-5}\ \text{sec}^{-1}$) to ($10\ \text{sec}^{-1}$). The authors pointed out that the yield strength is more rate-sensitive than the ultimate strength, and that the length of the plastic plateau is significantly affected by the strain-rate. Based on their experimental results, it is evident that different levels of rate-sensitivity should be considered for the plastic plateau and strain hardening ranges in order to predict the material response realistically, especially when large strains are involved. For con-

† Academic Visitor
‡ Lecturer in Engineering Computing

crete, Soroushian, *et al.* (1986) derived empirical expressions for the strain-rate effect on the compressive strength, the strain at maximum compressive strength, and the secant modulus of elasticity in compression. John and Shah (1987) concluded that the rate-sensitivity of concrete in tension is higher than in compression, and that the secant modulus of elasticity evaluated at the peak strength increases with the strain-rate. Fu, *et al.* (1991) reviewed the effects of loading rate on reinforced concrete members, and they suggested that the strain-rate effect may shift the failure mode from a ductile manner to a less desirable brittle mode.

In this paper, the three-parameter rate-sensitive material model, proposed in the companion paper (Izzuddin & Fang 1997), is extended to trilinear stress-strain relationships for concrete and steel. For concrete, two trilinear static stress-strain curves are employed for tension and compression respectively, which account for strain-softening in the tensile and compressive ranges. For steel, a trilinear static stress-strain relationship with kinematic strain-hardening is employed, which allows different levels of rate-sensitivity to be accounted for in the plastic plateau and the strain-hardening ranges. The implementation of the proposed models within an incremental-iterative solution procedure is discussed, with consideration given to the cases of elastic response, plastic loading and plastic unloading.

The paper provides verification of the trilinear steel model against available experimental results, where good agreement is observed. Several application examples of steel and reinforced concrete structures subjected to blast loading are also presented. The results confirm the importance of material rate-sensitivity on the overall dynamic response of steel and reinforced concrete structures, and emphasise the need for material models which can predict the strain-rate effect realistically.

2. Rate-sensitive concrete model

In this work, the static stress-strain relationship for concrete is assumed to be trilinear, both in tension and compression, as shown in Fig. 1. This allows material rate-sensitivity to be accounted for in the strain-softening range, which corresponds to the descending parts of the trilinear curves. The total strain-rate is decomposed into an elastic part $\dot{\varepsilon}_e$ and a plastic part $\dot{\varepsilon}_p$, where the various strains are shown in Fig. 2. The plastic strain-rate is dependent on the overstress (X) in accordance with visco-plastic theory:

$$\dot{\varepsilon}=\dot{\varepsilon}_e+\dot{\varepsilon}_p \tag{1}$$

$$E\,\dot{\varepsilon}_p=f\langle X\rangle \tag{2}$$

where (E) is the secant modulus of elasticity, denoted by (E_{st}) in tension or (E_{sc}) in compression. The rate-function $f\langle X\rangle$ is based on a three-parameter relationship between the steady-state overstress and strain-rate, as proposed in the companion paper (Izzuddin & Fang 1997):

$$X=SN\ln\left(1+\left\{\frac{\dot{\varepsilon}}{\dot{\varepsilon}*}\right\}^{1/N}\right) \tag{3}$$

In this model, a uniform steady-state overstress (X) is assumed over the whole of the strain-softening range, but with two different levels for tension and compression. Consequently, two sets of material constants (S), ($\dot{\varepsilon}*$) and (N) are employed for tension and compression, respectively,

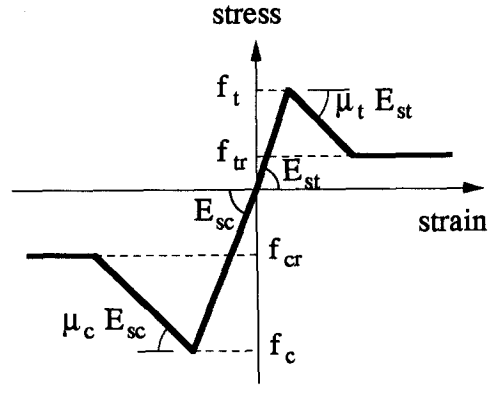

Fig. 1 Static stress-strain relationships for concrete.

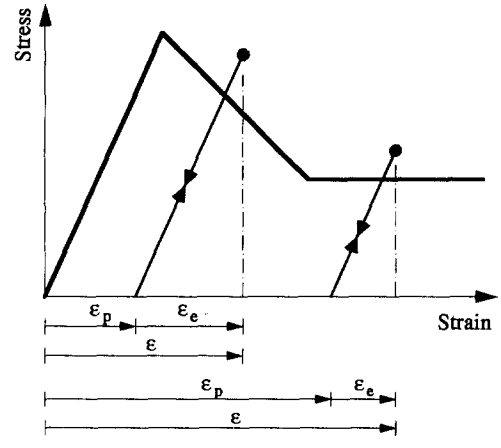

Fig. 2 Elastic and plastic strains for trilinear concrete model.

which may be determined from experimental data on the variation of overstress with strain-rate.

The above expression in Eq. (3) leads to the following rate-function (Izzuddin & Fang 1997):

$$f\langle X\rangle = E(1-\mu)\,\dot{\varepsilon} * (e^{X/SN}-1)^N \tag{4}$$

where (μ) is the strain-softening parameter, denoted by (μ_t) in tension or (μ_c) in compression (Fig. 1), taken as zero in the constant residual stress ranges.

As derived in the companion paper (Izzuddin & Fang 1997), the governing first-order differential equation is given by:

$$\dot{X} + f\langle X\rangle = E(1-\mu)\,\dot{\varepsilon} \tag{5}$$

This differential equation is integrated in the strain-softening tensile and compressive ranges using the single-step method proposed in the companion paper.

The static cyclic characteristics of the trilinear concrete model are shown in Fig. 3 for tension and compression. If the concrete is first subjected to tensile strains causing stresses beyond the maximum tensile strength (OAB or OAB'), then further compressive straining results in unloading and crack closure (BCO or B'C''O) before any compressive stresses can be sustained (OD).

On the other hand, if concrete is subjected to compressive strains causing stresses beyond the maximum compressive strength (ODE or OD'E'), then tensile stresses cannot be sustained upon further tensile straining (EFC or E'F'C). These characteristics are supported by general experimental observations.

Experimental evidence shows that the maximum tensile and compressive strengths of concrete increase with the strain-rate. Soroushian, *et al.* (1986) give the following empirical expression for the effect of strain-rate on the compressive strength of concrete:

$$X_c = f_c(0.48 + 0.160 \times \log_{10}(\dot{\varepsilon}) + 0.0127 \times (\log_{10}(\dot{\varepsilon}))^2) \tag{6a}$$

where (X_c) is the increase in the maximum compressive strength.

For concrete in tension, the least-square curve fitting method is used to obtain a similar expression based on the experimental results reported by John and Shah (1987):

$$X_t = f_t(1.23 + 0.404 \times \log_{10}(\dot{\varepsilon}) + 0.0351 \times (\log_{10}(\dot{\varepsilon}))^2) \tag{6b}$$

where (f_t) is the static maximum tensile strength, and (X_t) is the increase in the maximum tensile strength due to rate-sensitivity.

Assuming that the steady-state overstress is achieved before any plastic strains are induced, the relationship between the increase in maximum strength, (X_c) or (X_t), and the steady-state

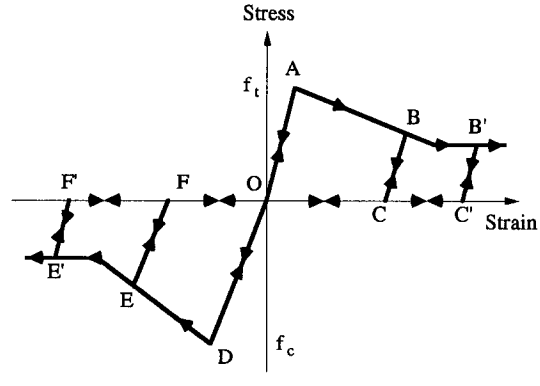

Fig. 3 Cyclic characteristics of trilinear concrete model.

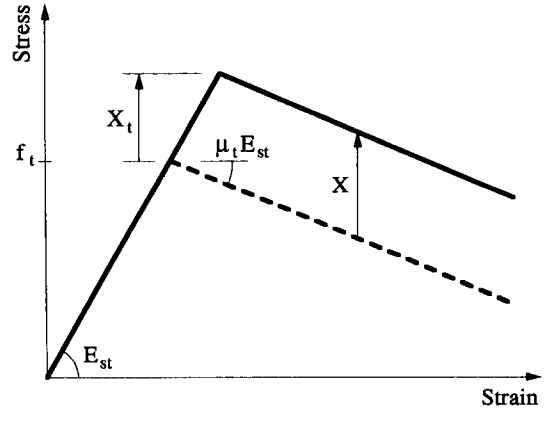

Fig. 4 Relationship between steady-state overstress and increase in maximum strength.

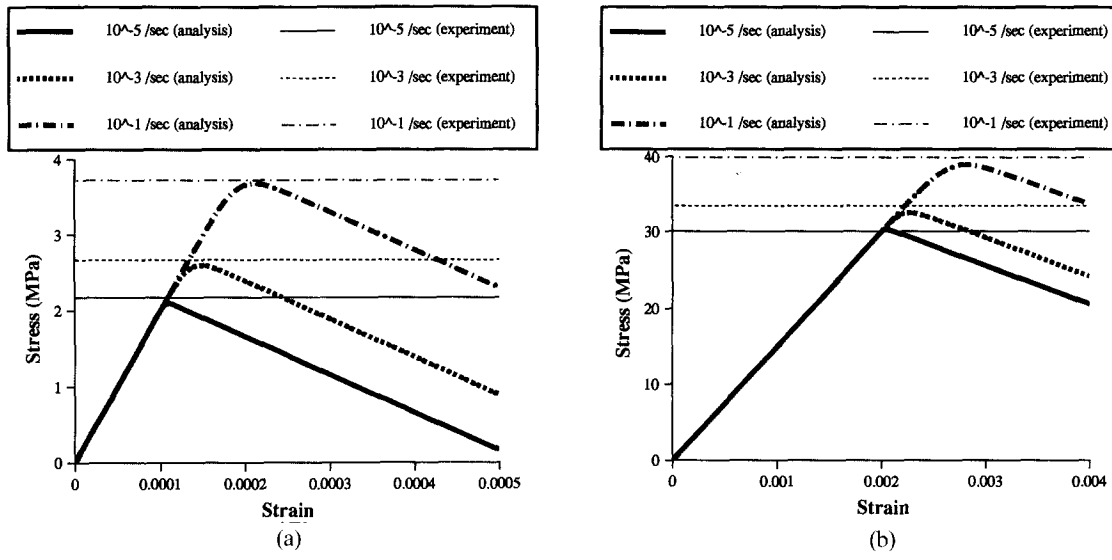

Fig. 5 (a) Maximum dynamic strength for concrete in tension. (b) Maximum dynamic strength for concrete in compression.

overstress (X) for a trilinear static stress-strain curve is given by:

$$X=(1-\mu_c)X_c \tag{7a}$$

$$X=(1-\mu_t)X_t \tag{7b}$$

where both (μ_c) and (μ_t) are negative. The above relationship is illustrated graphically in Fig. 4 for the tensile overstress.

The above expressions in Eqs. (6) and (7), for the steady state overstress in compression and tension, can be accurately fitted by the three-parameter relationship proposed in Eq. (3), the corresponding material constants being ($S=0.066(1-\mu_c)f_c$, $N=2$, $\dot{\varepsilon}*=6.66\times10^{-4}$ sec^{-1}) and ($S=0.14(1-\mu_t)f_t$, $N=2$, $\dot{\varepsilon}*=1.5\times10^{-4}$ sec^{-1}) for compression and tension, respectively.

The monotonic response of the proposed trilinear concrete model is illustrated in Fig. 5 for three constant strain-rates: (10^{-5} sec^{-1}), (10^{-3} sec^{-1}) and (10^{-1} sec^{-1}). These results are obtained using the above material constants for rate-sensitivity and the following static material constants ($E_{sc}=15000$ MPa, $f_c=30$ MPa, $\mu_c=0.333$, $f_{cr}=0$ MPa) for compression and ($E_{st}=20000$ MPa, $f_t=2$ MPa, $\mu_t=0.25$, $f_{tr}=0$ MPa) for tension. The dynamic stress-strain curves in Figs. 5a. and 5b demonstrate good agreement against the maximum dynamic strengths obtained from the experiments of Soroushian, *et al.* (1986) and John and Shah (1987).

3. Rate-sensitive steel model

Experimental evidence (Soroushian & Choi 1987) indicates that steel exhibits different levels of rate-sensitivity in the plastic plateau and the strain hardening ranges, and that the plastic plateau lengthens with higher strain-rates. To account for these phenomena, the rate-sensitive model proposed in the companion paper (Izzuddin & Fang 1997) is extended to a trilinear static stress-strain relationship (Fig. 6), where different rate-functions are employed in the plastic

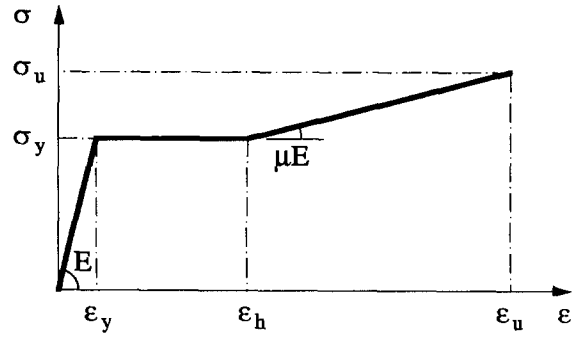

Fig. 6 Trilinear model for steel.

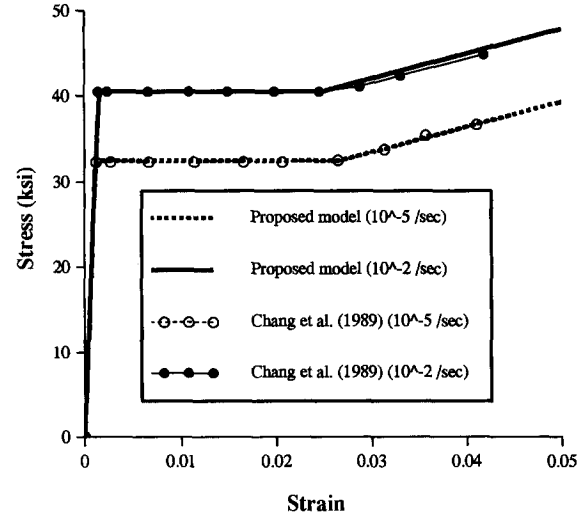

Fig. 7 Rate-sensitive response of mild steel at constant strain-rate.

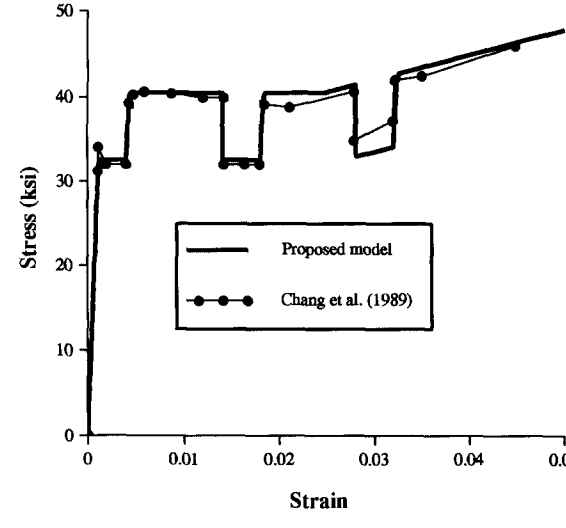

Fig. 8 Rate-sensitive response of mild steel at variable strain-rate.

plateau and the strain hardening ranges. In the former range the rate-function reflects the increase in the dynamic yield strength, whereas in the latter range the rate-function reflects the increase in the dynamic ultimate strength.

To demonstrate the accuracy of the proposed trilinear model, comparisons are undertaken in Figs. 7 and 8 against the experimental results by Chang, *et al.* (1989) for monotonic loading at constant strain-rates (10^{-5} sec^{-1} and 10^{-2} sec^{-1}) and at variable strain-rates between the same two limits. In these comparisons, the static material constants ($E=29000$ ksi, $\sigma_y=27$ ksi, $\varepsilon_h=0.0129$, $\mu=0.01$) are used; the material constant for rate-sensitivity are ($S=2.87$ ksi, $\dot{\varepsilon}*=3.54\times10^{-3}$ sec^{-1}, $N=6$) for the plastic plateau range and ($S=1.303$ ksi, $\dot{\varepsilon}*=4.467\times10^{-6}$ sec^{-1}, $N=1$) for the strain-hardening range. The trilinear model is shown to predict with good accuracy the rate-sensitive response under both constant and variable strain-rates and for both the plastic plateau and strain-hardening ranges.

4. Implementation

The proposed trilinear models are implemented within the nonlinear analysis program ADAPTIC (Izzuddin 1991), thus enabling the large displacement analysis of steel and reinforced concrete frames subjected to severe dynamic loading. As discussed in the companion paper (Izzuddin & Fang 1997), the cubic beam-column formulation utilising the proposed models requires the calculation of the current stress (σ_1) corresponding to the current strain (ε_1), as well as the determination of a tangent modulus (E_t).

The main distinction between the trilinear concrete and steel models is in the static stress-strain relationship for the plastic range $g(E)$. For the trilinear concrete model (Fig. 1), the tensile relationship $g(\varepsilon)$ is given by:

$$g(\varepsilon)=\begin{cases}(1-\mu_t)f_t-\mu_t E_{st}\varepsilon, & \text{if } \varepsilon<\dfrac{(1-\mu_t)f_t-f_{tr}}{\mu_t E_{st}}\\ f_{tr}, & \text{if } \varepsilon\geq\dfrac{(1-\mu_t)f_t-f_{tr}}{\mu_t E_{st}}\end{cases} \tag{8}$$

with a similar relationship for the compressive $g(\varepsilon)$.

On the other hand, the tensile relationship $g(\varepsilon)$ for the trilinear steel model (Fig. 6) is given by:

$$g(\varepsilon)=\begin{cases}\sigma_y, & \text{if } \varepsilon<\varepsilon_h\\ \sigma_y+\mu E(\varepsilon-\varepsilon_h), & \text{if } \varepsilon\geq\varepsilon_h\end{cases} \tag{9}$$

with an almost identical relationship in compression.

Another important distinction between the trilinear concrete and steel models is in the rate-functions. The concrete model is based on two different rate-functions for tension and compression, but no distinction is made between the descending and horizontal branches of a particular strain-softening range. The steel model, on the other hand, employs the same rate-functions in tension and compression, but uses two different functions for the plastic plateau and strain-hardening ranges.

The implementation of the two models is described hereafter with reference to a general piecewise linear curve for static tensile plasticity, with the treatment of compressive plasticity being

almost identical. Three cases are discussed in the following sections, which deal with stress and tangent modulus calculation in the elastic and plastic ranges.

4.1. Elastic response

When the previous state is elastic ($g(\varepsilon_0)>\sigma_0$), the current stress ($\sigma_1$) is obtained from the current strain (ε_1) assuming, in the first instance, a fully elastic response:

$$\sigma_1=\sigma_0+E(\varepsilon_1-\varepsilon_0) \tag{10}$$

If the current state is elastic ($g(\varepsilon_1)\geq\sigma_1$), then the stress obtained from Eq. (10) is accepted, and the tangent modulus (E_t) is taken to be identical to (E). However, if the current state is plastic ($g(\varepsilon_1)<\sigma_1$), the strain ($\varepsilon_c$) at which the elastic loading curve intersects the static plastic curve is first determined from the solution of the equation:

$$\sigma_0+E(\varepsilon_c-\varepsilon_0)=g(\varepsilon_c) \tag{11}$$

The remainder of the strain increment ($\varepsilon_1-\varepsilon_c$) leads to plastic loading, where the calculation of the current stress and tangent modulus can be performed in accordance with the following section assuming ($\varepsilon_0=\varepsilon_c$), ($\sigma_0=g(\varepsilon_c)$) and ($X_0=0$), and scaling ($\Delta t$) to maintain the original strain-rate.

4.2. Plastic loading

When the previous state is plastic ($g(\varepsilon_0)\leq\sigma_0$), the determination of the current state depends on the direction of straining. For tensile plasticity, plastic loading is associated with a positive strain-rate ($\dot{\varepsilon}\geq 0$), taken to be constant during the incremental step:

$$\dot{\varepsilon}=\frac{\varepsilon_1-\varepsilon_0}{\Delta t} \tag{12}$$

Given the previous overstress (X_0), the current overstress (X_1) can be calculated using the single-step numerical integration procedure proposed in the companion paper (Izzuddin & Fang 1997). It is noted that this numerical integration procedure should be applied with a single rate-function over the incremental step. For the trilinear steel model with ($\varepsilon_0<\varepsilon_h$) and ($\varepsilon_1>\varepsilon_h$), the rate-function changes as the strain exceeds (ε_h); in such a case, the strain increment is applied in two steps ($\varepsilon_0\rightarrow\varepsilon_h$) and ($\varepsilon_h\rightarrow\varepsilon_1$), each being associated with a different rate-function. Once the current overstress (X_1) is obtained, the current stress (σ_1) is determined from:

$$\sigma_1=g(\varepsilon_1)+X_1 \tag{13}$$

The tangent modulus (E_t) for this case is obtained from the following expression:

$$E_t=\frac{d\sigma_1}{d\varepsilon_1}=\frac{dg(\varepsilon_1)}{d\varepsilon_1}+\frac{1}{\Delta t}\frac{dX_1}{d\dot{\varepsilon}} \tag{14}$$

where the calculation of the derivative of (X_1) with respect to ($\dot{\varepsilon}$) is described in the companion paper (Izzuddin & Fang 1997).

4.3. Plastic unloading

For the case of a previous tensile plastic state ($g(\varepsilon_0) \leq \sigma_0$), plastic unloading is associated with a negative strain-rate ($\dot{\varepsilon}<0$), as depicted in Fig. 9. The governing nonlinear visco-plastic differential equation, which is given by (Izzuddin & Fang 1997):

$$\dot{X}+E(1-\mu)\,\dot{\varepsilon}*(e^{X/SN}-1)^N=E(1-\mu)\,\dot{\varepsilon} \tag{15}$$

is approximated linearly using a secant approach, as shown in Fig. 10. The resulting linear differential equation is expressed by:

$$\dot{X}+a_s X=E(1-\mu)\dot{\varepsilon} \tag{16a}$$

where,

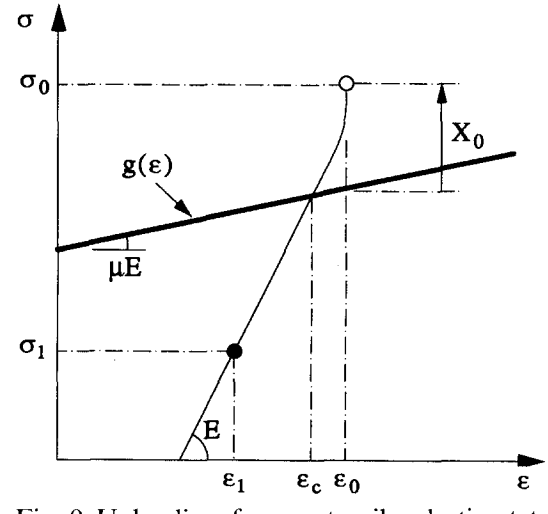

Fig. 9 Unloading from a tensile plastic state.

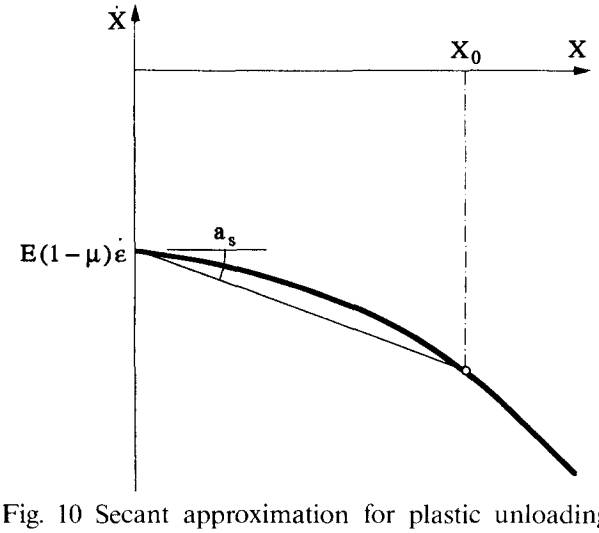

Fig. 10 Secant approximation for plastic unloading.

$$a_s = \frac{E(1-\mu)\dot{\varepsilon}*}{X_0}\left(e^{X_0/SN}-1\right)^N \tag{16b}$$

The current overstress (X_1) can be obtained from the solution of the above differential equation:

$$X_1 = \left(X_0 - \frac{E(1-\mu)\dot{\varepsilon}}{a_s}\right)e^{-a_s\Delta t} + \frac{E(1-\mu)\dot{\varepsilon}}{a_s} \tag{17}$$

which can be used to determine the current stress (σ_1) according to Eq. (13). The tangent modulus (E_t) can also be obtained from Eq. (14).

It is noted that the expression for (X_1) in Eq. (17) is only valid for ($X_1 \geq 0$). If the current overstress is negative, then elastic unloading occurs, as depicted in Fig. 10 for a current strain (ε_1) less than the critical strain (ε_c). The critical strain (ε_c) corresponds to a zero overstress, and can be determined from the critical time-step (Δt_c) using Eq. (17):

$$\Delta t_c = -\frac{1}{a_s} ln\left(\frac{E(1-\mu)\dot{\varepsilon}}{E(1-\mu)\dot{\varepsilon} - a_s X_0}\right) \tag{18a}$$

$$\varepsilon_c = \varepsilon_0 + \dot{\varepsilon}\Delta t_c \tag{18b}$$

In the case of elastic unloading, the calculation of the current stress and tangent modulus can be performed in accordance with Section 6.1, assuming ($\varepsilon_0 = \varepsilon_c$) and ($\sigma_0 = g(\varepsilon_c)$).

5. Application

Several examples are presented hereafter to demonstrate the applicability of the proposed steel and concrete rate-sensitive models. In this regard, ADAPTIC v2.5.1 (Izzuddin 1991) is used to undertake nonlinear dynamic analysis of the steel and reinforced concrete structures under consideration.

5.1. Steel beam

The steel *I*-beam shown in Fig. 11 is identical to the last example in the companion paper (Izzuddin & Fang 1997), but is subjected to a larger amplitude blast loading with a shorter duration. The problem symmetry is utilised, where half of the beam is modelled using 10 elasto-plastic cubic elements with appropriate boundary conditions. In obtaining the dynamic response of the beam, both the bilinear and trilinear rate-sensitive models are used for comparison purposes. The experimental results of Soroushian and Choi (1987) are fitted by the trilinear model, where two sets of rate-function parameters are employed, ($S = 6.6$ MPa, $\dot{\varepsilon}* = 4\times10^{-9}$ sec^{-1}, $N = 5$) and ($S = 8.52$ MPa, $\dot{\varepsilon}* = 1.1\times10^{-3}$ sec^{-1}, $N = 1$), for the plastic plateau and strain-hardening ranges, respectively. For the bilinear model, the rate-function parameters corresponding to the plastic plateau range are employed.

Comparison of the results in Fig. 12 demonstrates the importance of realistic material modelling, where it is shown that the bilinear rate-sensitive model predicts a maximum midspan displacement which is (24%) smaller than that predicted by the trilinear model. This is expected, since the bilinear model assumes that strain-hardening commences immediately after yielding, and hence does not account for the plastic plateau. Nevertheless, it is possible that a reduction in the

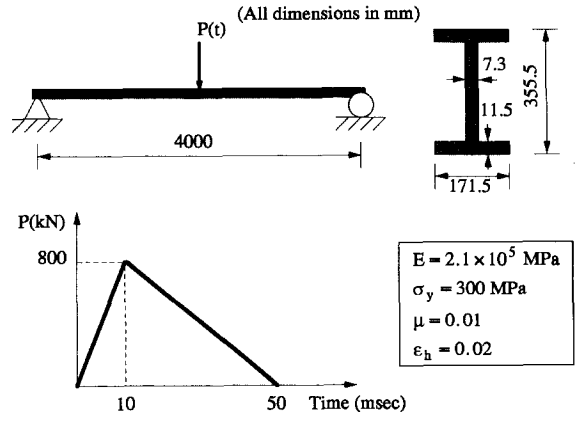

Fig. 11 Geometric configuration and loading of steel *I*-beam.

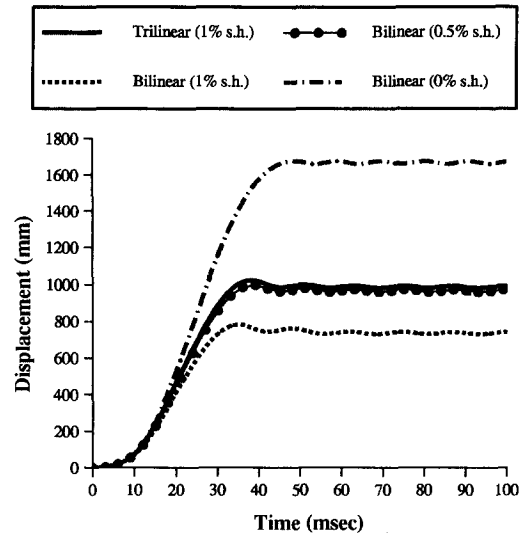

Fig. 12 Effect of material model on response prediction of *I*-beam.

strain-hardening parameter (μ) for the bilinear model could lead to improved accuracy, as illustrated in Fig. 12 for the reduced value (μ=0.5%). However, the appropriate choice of (μ) for the bilinear model depends on the particular problem and the severity of the applied loading.

5.2. Steel frame

The multi-storey steel frame shown in Fig. 13 is subjected to a concentrated blast load at the mid-height of an internal second storey column. The blast load varies according to the same triangular pulse employed in the previous example, but with a peak value of (4000 kN). This value represents twice the static column capacity obtained with the assumption of full rotational restraint at the two ends.

The response of the frame is obtained using adaptive analysis (Izzuddin & Elnashai 1993), where the analysis is started with one elastic element per member, and elasto-plastic cubic elements

are introduced only when material plasticity is detected. The same material models used in the previous examples are employed here for the elasto-plastic elements, with three cases being considered: trilinear model with rate-sensitivity (***T-R***), bilinear model with rate-sensitivity (***B-R***) and trilinear model without rate-sensitivity (***T-I***). The results shown in Fig. 14 for the mid-height column displacement demonstrate again the importance of realistic material modelling, where the bilinear rate-sensitive model (***B-R***) predicts a maximum displacement which is (32%) smaller than that of the trilinear rate-sensitive model (***T-R***). The effect of ignoring rate-sensitivity (***T-I***) is associated with a (68%) increase in the maximum displacement.

The choice of the material model also influences the spread of plasticity within the frame, which can be quantified here by means of highlighting the mesh of elasto-plastic cubic elements. It is observed from Figs. 15a and 15b, that the spread of plasticity is similar for the bilinear and trilinear rate-sensitive models except in the immediate vicinity of the load, with the bilinear model leading to a wider spread of plasticity in the beams and an opposite effect in the columns. The inclusion of material rate-sensitivity also leads to more plasticity in the far columns and less plasticity in the far beams, as demonstrated in the comparison of Figs. 15a and 15c.

5.3. Reinforced concrete beam

The response of the simply supported beam shown in Fig. 16 to uniform blast pressure was studied experimentally by Allgood and Swihart (1970). In these experiments, a constant long duration pressure was applied, having an amplitude equal to the static ultimate load (p_u=0.156 MPa (22.6 psi)), and achieving the full value over a very small rise-time.

The problem symmetry is utilised, where half of the beam is modelled using 12 elasto-plastic cubic elements with appropriate boundary conditions. Since Allgood and Swihart (1970) did not undertake direct experiments on the steel and concrete materials, the material rate-sensitivity is approximated using the results of other experimental work. The expressions of John and

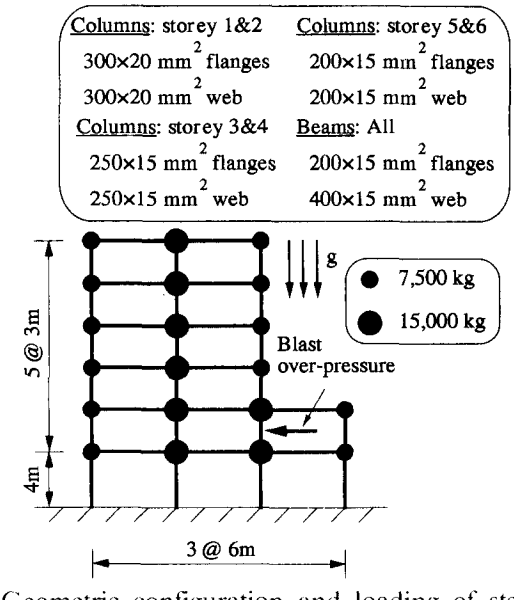

Fig. 13 Geometric configuration and loading of steel frame.

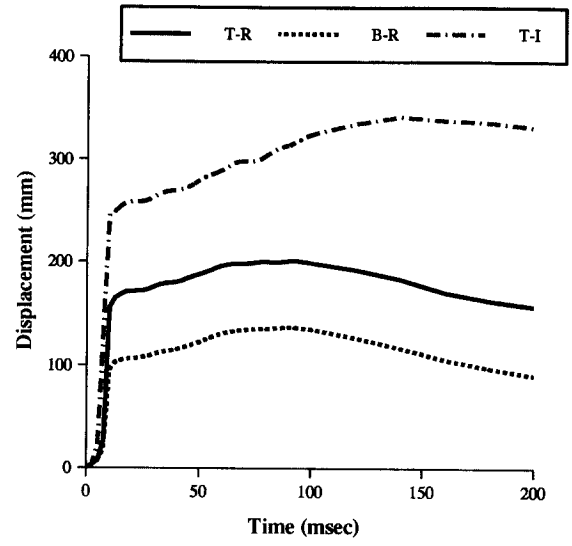

Fig. 14 Response of steel frame at point of loading.

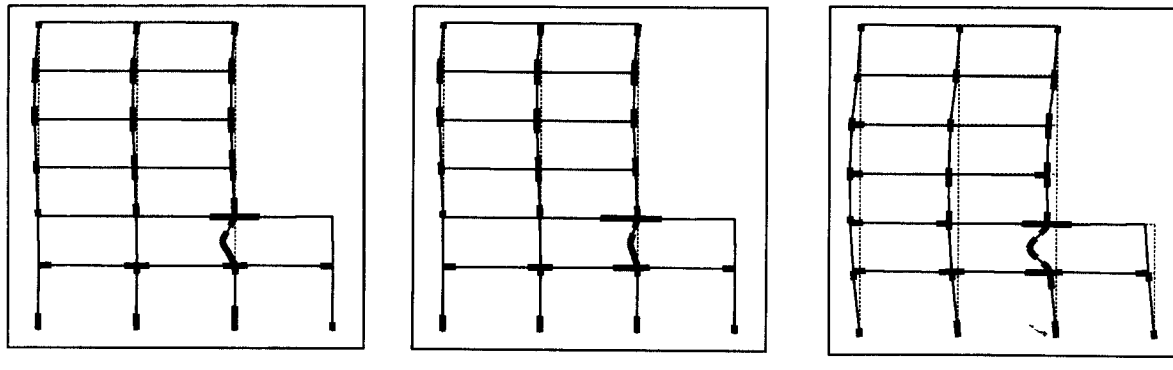

(a) Trilinear rate-sensitive model: ***T-R***

(b) Bilinear rate-sensitive model: ***B-R***

(c) Trilinear rate-insensitive model: ***T-I***

Fig. 15 Final deflected shapes (scale=5) and spread of plasticity for steel frame.

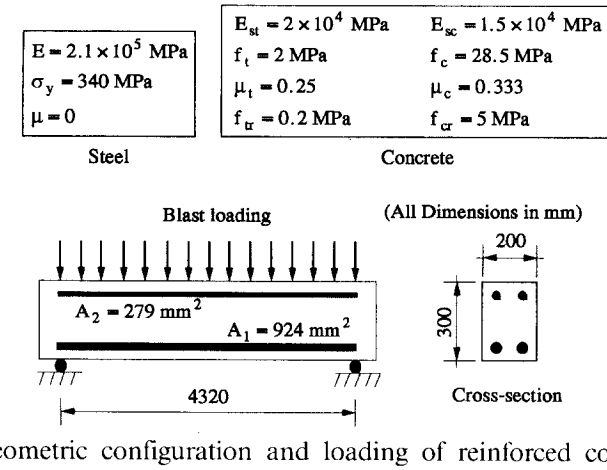

Fig. 16 Geometric configuration and loading of reinforced concrete beam.

Shah (1987) and Soroushian, *et al.* (1986) are used to determine the rate-sensitivity parameters for concrete, where the parameters (S=0.35 MPa, $\dot{\varepsilon}*=1.5\times10^{-4}$ sec^{-1}, N=2) are used for tension and (S=2.51 MPa, $\dot{\varepsilon}*=6.66\times10^{-4}$ sec^{-1}, N=2) are used for compression. For the steel reinforcement, the bilinear model is employed, with three levels of rate-sensitivity being considered; the first (***R1***), (S=6 MPa, $\dot{\varepsilon}*=5\times10^{-5}$ sec^{-1}, N=1), is based on fitting the CEB (1988) expression; the second (***R2***), (S=3 MPa, $\dot{\varepsilon}*=5\times10^{-5}$ sec^{-1}, N=1) represents a (50%) reduction in rate-sensitivity over (***R1***); and the third (***R3***), (S=3 MPa, $\dot{\varepsilon}*=5\times10^{-4}$ sec^{-1}, N=1), represents a further reduction in rate-sensitivity over (***R2***).

The response of the beam to the full pressure (p_u) is depicted in Fig. 17, where the second level of steel rate-sensitivity (***R2***) is in excellent agreement with the maximum displacement of (86 mm) recorded by Allgood and Swihart (1970). However, in the absence of experimental data on the material response, it remains unclear whether such agreement is due to (***R2***) representing accurately the rate-sensitive characteristics of the steel reinforcement. Nevertheless, this example illustrates again the importance of accounting for material rate-sensitivity, since the rate-insensitive response would predict collapse of the beam under the full pressure loading (p_u).

5.4. R/C frame

The four-storey reinforced concrete frame, shown in Fig. 18, is subjected to an external blast load, which varies according to the same triangular pulse used in the first two examples but with a peak value of (4500 kN). All columns are assumed to have a square cross-section with one layer of steel reinforcement bars at a cover distance of (2.5 cm) on each side of the cross-section. Geometric and reinforcement details of the columns are given in Table 1. With reference to Fig. 18, all beams have a rectangular cross-section and a varying reinforcement layout, with the details as given in Table 2. The two reinforcement layers are placed at a cover distance of (5 cm). Gravity loads are assumed to be applied at the structure nodes, with the details of the corresponding masses given in Table 3.

The bilinear model is used for the steel reinforcement, with the static material constants (E=2.1 $\times10^5$ MPa, σ_y=300 MPa, μ=0.005) and the rate-sensitivity constants (S=6.6 MPa, $\dot{\varepsilon}*=4\times10^{-9}$

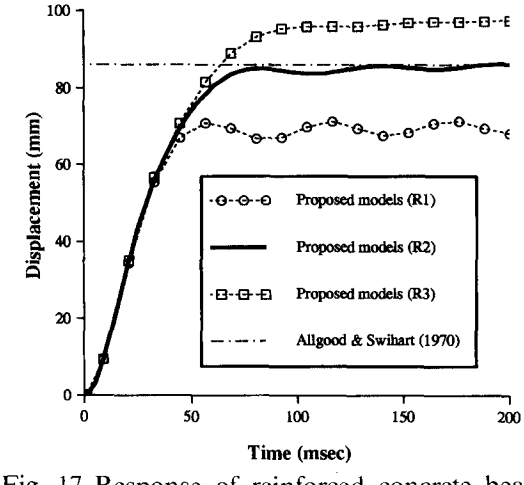

Fig. 17 Response of reinforced concrete beam.

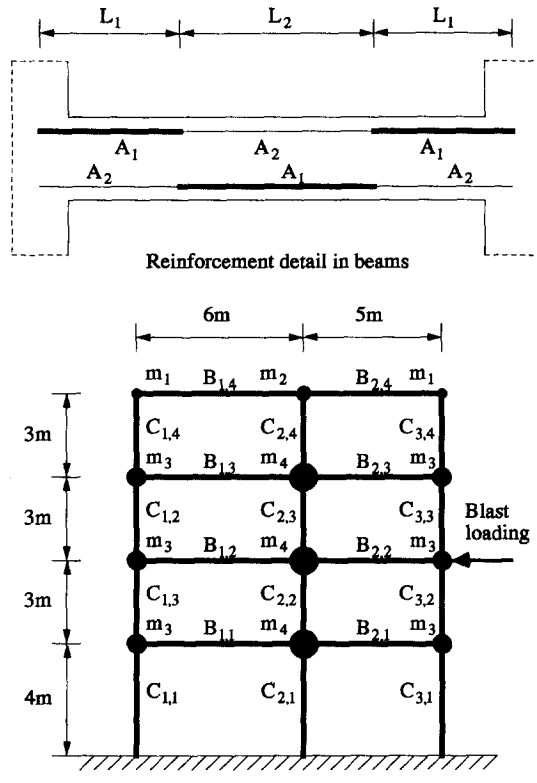

Fig. 18 Geometric configuration and loading of reinforced concrete frame.

Table 1 Cross-sectional details of columns

Column	Size (cm×cm)	Reinforcement/side
$C_{1,1}$	45×45	8ϕ18
$C_{1,2}$	45×45	6ϕ18
$C_{1,3}$	45×45	6ϕ16
$C_{1,4}$	45×45	4ϕ16
$C_{2,1}$	50×50	8ϕ20
$C_{2,2}$	50×50	6ϕ20
$C_{2,3}$	50×50	6ϕ18
$C_{2,4}$	50×50	4ϕ18
$C_{3,1}$	40×40	6ϕ20
$C_{3,2}$	40×40	4ϕ20
$C_{3,3}$	40×40	4ϕ18
$C_{3,4}$	40×40	4ϕ16

sec^{-1}, $N=5$). For concrete, the trilinear model is used with the same material properties as were used in the previous example, except for the two compressive properties ($f_c=30$ MPa, $S=2.64$ MPa). The response at the point of loading in Fig. 19 demonstrates that ignoring the material rate-sensitivity leads to a (100%) increase in the maximum predicted displacement. The material response for concrete and reinforcement steel at the top of column ($C_{3,2}$), shown in Figs. 20a and 20b, exhibits a considerable reduction in the material strains with a significant increase

Table 2 Cross-sectional and reinforcement details of beams

Beam	Size (cm×cm)	A_1	A_2	L_1/L_2
$B_{1,1}$	30×60	6φ18	2φ18	3/4
$B_{1,2}$	30×60	6φ18	2φ18	3/4
$B_{1,3}$	30×60	6φ18	2φ18	3/4
$B_{1,4}$	30×60	6φ18	2φ18	3/4
$B_{2,1}$	25×60	6φ16	2φ16	3/4
$B_{2,2}$	25×60	6φ16	2φ16	3/4
$B_{2,3}$	25×60	6φ16	2φ16	3/4
$B_{2,4}$	25×60	6φ16	2φ16	3/4

Table 3 Nodal masses

Mass no.	Mass ($\times 10^3$ kg)
m_1	5.10
m_2	7.65
m_3	10.19
m_4	15.29

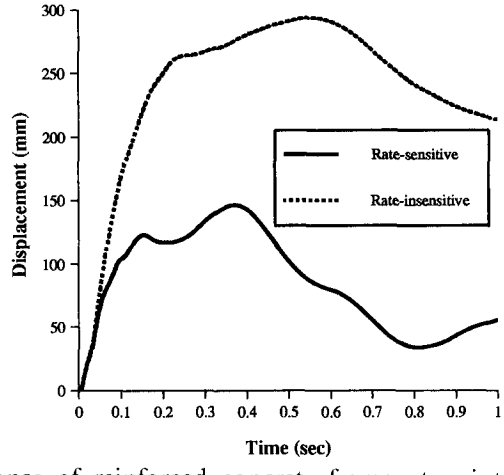

Fig. 19 Response of reinforced concrete frame at point of loading.

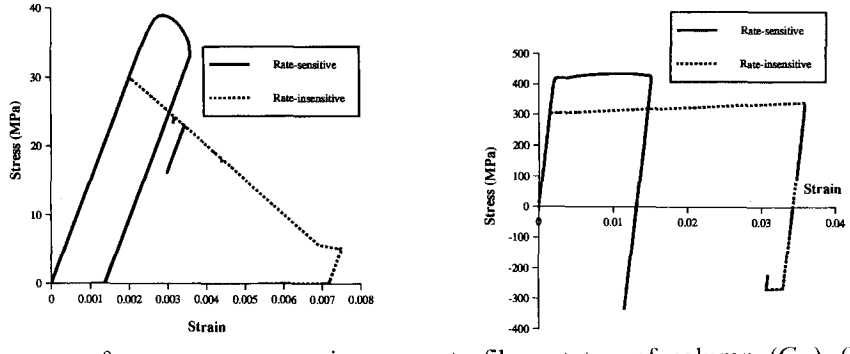

Fig. 20 (a) Response of extreme compressive concrete fibre at top of column ($C_{3,2}$). (b) Response of tensile steel reinforcement at top of column ($C_{3,2}$).

in the material stresses when rate-sensitivity is accounted for.

6. Conclusions

The companion paper presents a new rate-sensitive material model employing a three-parameter rate-function and based on a bilinear static stress-strain relationship. This paper extends the basic bilinear model to cover trilinear static stress-strain relationships for steel and concrete; discusses the implementation of the proposed trilinear models; and presents examples of their applicability to the nonlinear analysis of steel and reinforced concrete structures subjected to severe dynamic loading.

The paper first discusses the trilinear concrete model, where rate-sensitivity is accounted for in the strain-softening range, and different rate-function parameters are employed in tension and compression. In this regard, the use of the three-parameter rate-function proposed in the companion paper allows the fitting of various experimental results with good accuracy.

The trilinear steel model is also described, where different levels of rate-sensitivity are employed in the plastic plateau and strain-hardening ranges. It is shown that the proposed trilinear model enables more accurate representation of experiments at constant and variable strain-rates than the basic bilinear model.

The implementation of the proposed models is outlined with reference to a general piecewise linear plastic curve, where the cases of elastic response, plastic loading and plastic unloading are considered. Several application examples are then presented, which demonstrate the importance of rate-sensitivity in the prediction of the dynamic response of steel and reinforced concrete structures. It is observed that the trilinear steel model leads to a considerably larger response than the bilinear steel model with similar rate-sensitivity and strain-hardening parameters. In view of this, it is recommended that the trilinear steel model should be used in order to account for different rate-sensitivity in the plastic plateau and strain-hardening ranges. In addition, it is suggested that further experimental investigation into the rate-sensitivity of steel and concrete is needed to facilitate the calibration of rate-sensitive material models and the choice of appropriate model parameters.

Acknowledgements

The authors gratefully acknowledge the financial support provided by the British Council for the first author through the Technical Cooperation Award.

References

Allgood, J.R. and Swihart, G.R. (1970), "Design of flexural members for static and blast loading", *ACI Monograph*, No. 5, Detroit, Michigan, 43-44.

Chang, K.C., Sugiura, K. and Lee, G.C. (1989), "Rate-dependent material model for structural steel", *Journal of Engineering Mechanics, ASCE*, **115**(3), 465-474.

CEB, (1988), "Structures under impact and impulsive loading", *Bulletin d'Information* No. 187, Comite Euro-International de Beton, CEB.

Fu, H.C., Erki, M.A. and Seckin, M. (1991), "Review of effects of loading rate on reinforced concrete", *Journal of Structural Engineering, ASCE,* **117**(12), 3660-3679.

Izzuddin, B.A. (1991), "Nonlinear dynamic analysis of framed structures", PhD thesis, Civil Engineering Department, Imperial College, London, U.K.

Izzuddin, B.A. and Elnashai, A.S. (1993), "Adaptive space frame analysis. Part II: Distributed plasticity approach", *Proceedings of the Institution of Civil Engineers, Structures and Buildings,* **99**, 317-326.

Izzuddin, B.A. and Fang, Q. (1997), "Rate-sensitive analysis of framed structures. Part I: Model formulation and verification", *Structural Engineering and Mechanics, An Int'l Journal,* **5**(3), 221-238.

John, R. and Shah, S.P. (1987), "Constitutive modelling of concrete under impact loading", *Proceedings of the First International Conference on the Effects of Fast Transient Loadings,* W.J. Ammann, *et al.* (eds.), 37-65.

Soroushian, P., Choi, K. and Alhamad, A. (1986), "Dynamic constitutive behavior of concrete", *ACI Journal,* **83**(2), 251-258.

Soroushian, P. and Choi, K. (1987), "Steel mechanical properties at different strain rates", *Journal of Structural Engineering, ASCE,* **113**(4), 663-673.